

PLF-1 (Proliferin-1) Modulates Smooth Muscle Cell Proliferation and Development of Experimental Intimal Hyperplasia

Lina Hu, MD, PhD;* Zhe Huang, MD, PhD;* Hideki Ishii, MD, PhD; Hongxian Wu, MD, PhD; Susumu Suzuki, MD, PhD; Aiko Inoue, PhD; Weon Kim, MD, PhD; Haiying Jiang, PhD; Xiang Li, MD, PhD; Enbo Zhu, MD, PhD; Limei Piao, MD, PhD; Guangxian Zhao, MD, PhD; Yanna Lei, MD, PhD; Kenji Okumura, MD, PhD; Guo-Ping Shi, DSc; Toyooki Murohara, MD, PhD; Masafumi Kuzuya, MD, PhD; Xian Wu Cheng, MD, PhD, FAHA

Background—Although apoptosis and cell proliferation have been extensively investigated in atherosclerosis and restenosis postinjury, the communication between these 2 cellular events has not been evaluated. Here, we report an inextricable communicative link between apoptosis and smooth muscle cell proliferation in the promotion of vascular remodeling postinjury.

Methods and Results—Cathepsin K–mediated caspase-8 maturation is a key initial step for oxidative stress–induced smooth muscle cell apoptosis. Apoptotic cells generate a potential growth-stimulating signal to facilitate cellular mass changes in response to injury. One downstream mediator that cathepsin K regulates is PLF-1 (proliferin-1), which can potently stimulate growth of surviving neighboring smooth muscle cells through activation of PI3K/Akt/p38MAPK (phosphatidylinositol 3-kinase/protein kinase B/p38 mitogen-activated protein kinase)-dependent and -independent mTOR (mammalian target of rapamycin) signaling cascades. We observed that cathepsin K deficiency substantially mitigated neointimal hyperplasia by reduction of Toll-like receptor-2/caspase-8–mediated PLF-1 expression. Interestingly, PLF-1 blocking, with its neutralizing antibody, suppressed neointima formation and remodeling in response to injury in wild-type mice. Contrarily, administration of recombinant mouse PLF-1 accelerated injury-induced vascular actions.

Conclusions—This is the first study detailing PLF-1 as a communicator between apoptosis and proliferation during injury-related vascular remodeling and neointimal hyperplasia. These data suggested that apoptosis-driven expression of PLF-1 is thus a novel target for treatment of apoptosis-based hyperproliferative disorders. (*J Am Heart Assoc.* 2019;8:e005886. DOI: 10.1161/JAHA.117.005886.)

Key Words: hyperplasia • proliferation • vascular remodeling • vascular smooth muscle

Despite significant improvements in endovascular therapy techniques, restenosis remains the principal limitation of coronary angioplasty.¹ Vascular media smooth muscle cell (SMC)-derived neointimal formation was originally considered to be the primary mechanism of restenosis after angioplasty.² A neointimal cellular mass at the vascular damage site was

shown to depend on the balance between cell proliferation and cell loss, including apoptosis.³ Although cell apoptosis and proliferation have been extensively investigated as independent contributors after balloon injury,^{3–6} the communication between apoptosis and cell proliferation in vascular remodeling and restenosis has been unclear. During the last

From the Department of Public Health, Guilin Medical College, Guilin, Guangxi, China (L.H.); Department of Cardiology/Hypertension and Heart Center, Yanbian University Hospital, Yanji, Jilin, China (L.H., X.L., E.Z., L.P., G.Z., Y.L., X.W.C.); Departments of Community & Geriatrics (L.H., A.I., L.P., M.K., X.W.C.) and Cardiology (H.I., S.S., K.O., T.M.), Nagoya University Graduate School of Medicine, Nagoya, Japan; Department of Neurology, Occupational and Environmental Health, Kitakyushu, Hukuoka, Japan (Z.H.); Department of Cardiology, Shanghai General Hospital, Shanghai Jiao Tong University School of Medicine, Shanghai, China (H.W.); Division of Cardiology, Department of Internal Medicine, Kyung Hee University, Seoul, South Korea (W.K., X.W.C.); Department of Physiology and Pathophysiology, Yanbian University School of Medicine, Yanji, Jilin, China (H.J.); Department of Cardiovascular Medicine, Brigham and Women's Hospital and Harvard Medical School, Boston, MA (G.-P.S.); Institute of Innovation for Future Society, Nagoya University, Nagoya, Japan (A.I., M.K., X.W.C.).

*Dr Hu and Dr Huang contributed equally to this study.

Correspondence to: Xian Wu Cheng, MD, PhD, FAHA, Department of Cardiology/Hypertension and Heart Center, Yanbian University Hospital, Juzijie 1327, Yanji, Jilin 133000, China or Institute of Innovation for Future Society, Nagoya University Graduate School of Medicine, 65 Tsuruma-cho, Showa-ku, Nagoya 466-8550, Japan. E-mails: chengxw0908@163.com or xianwu@med.nagoya-u.ac.jp

Received February 15, 2017; accepted March 22, 2018.

© 2019 The Authors. Published on behalf of the American Heart Association, Inc., by Wiley. This is an open access article under the terms of the Creative Commons Attribution-NonCommercial License, which permits use, distribution and reproduction in any medium, provided the original work is properly cited and is not used for commercial purposes.

Clinical Perspective

What Is New?

- Cathepsin K–mediated caspase-8 activation regulates smooth muscle cell apoptosis in response to oxidative stress.
- Apoptotic cells generate a potential PLF-1 (proliferin-1)-mediated growth-stimulating signal to facilitate cellular mass changes in response to injury.
- PLF-1–neutralizing antibody improved cellular mass formation and remodeling in wild-type mice.
- Administration of PLF-1 accelerated injury-related vascular response.

What Are the Clinical Implications?

- One downstream mediator that cathepsin K regulates is PLF-1, which can potently stimulate the growth of neighborhood surviving vascular smooth muscle cells by activation of PI3K/Akt/p38MAPK (phosphatidylinositol 3-kinase/protein kinase B/p38 mitogen-activated protein kinase)-dependent and -independent mTOR (mammalian target of rapamycin) signaling pathways.
- Apoptosis-driven expression of PLF-1 is thus a novel target for the treatment of apoptosis-based hyperproliferative disorders.

5 years, cancer studies demonstrated that dying cells use the apoptotic process to generate growth factors such as prostaglandin E₂ and hepatocyte growth factor to activate the repopulation of neoplasms after cytotoxic therapies.^{7,8} Thus, a better understanding of the interaction between apoptosis and cell proliferation could lead to therapies that improve the efficacy of antiproliferative drugs including stent-eluting compounds.

Cathepsins were originally identified as members of the cysteine protease family localized in the lysosomes.⁹ Over the past decade, emerging data revealed unexpected roles of cathepsins in pathological conditions such as tumors, bone disorders, and cardiovascular disease.^{10–14} Among the cathepsin family members, cathepsin K (CatK) was the first cathepsin found to be expressed in human atherosclerotic lesions.¹⁵ We first showed an increased expression of CatK in neointimal lesions of rat balloon-injured arteries in 2004.¹⁶ CatK ablation was shown to mitigate high-fat-diet–induced cardiomyocyte apoptosis and cardiac hypertrophy.¹⁷ Genetic and pharmacological interventions targeting CatK ameliorated injury-related vascular remodeling through the ability of CatK to stimulate SMC proliferation.⁴ However, CatK activation-mediated interaction between cell apoptosis and proliferation in the restenosis process after angioplasty is largely unknown.

Previous studies have shown that expression of Toll-like receptor (TLR), in particular TLR1, TLR2, and TLR4, is markedly

augmented in human and animal atherosclerotic lesions.^{18,19} TLR2 has been shown to be involved in inflammation-related atherosclerotic plaque growth and vascular remodeling.^{20–22} It was reported that on ligand binding, TLR activated p38MAPK (p38 mitogen-activated protein kinase) and Erk1/2 (extracellular signal-regulated kinase 1/2) signaling during SMC migration.²² TLR2 was also reported to regulate SMC apoptosis through a caspase-8–dependent mechanism.²⁰ It has been reported that caspase-8 plays an essential role in TLR2 and nuclear factor κ B in the B-cell apoptotic process.²³

Mitogen-regulated proteins (MRFs; also called proliferin [PLFs]) of the prolactin growth hormone family are expressed by the placenta in mid-gestation.²⁴ The PLFs comprise a group of 4 homologous proteins (PLF-1, PLF-2, PLF-3, and PLF-related protein). In 1988, M6PR (mannose-6-phosphate receptor) was characterized by Nelson et al as the PLF receptor.²⁵ Laboratory investigations have led to a number of important observations that contribute to a greater understanding of PLF. For example, reactivation of PLF gene expression was observed to be associated with increased angiogenesis in fibrosarcoma tumor progression.²⁶ PLF-1 has been shown to induce endothelial cell migration by G-protein-coupled, p38MAPK signaling activation.²⁷ PLF-1 was also required for Wnt and Notch activation in Musashi1-mediated progenitor cell expansion.²⁸ A previous study demonstrated that PLF-1 acts as an autocrine regulator of endothelial cell proliferation in angiogenesis.²⁹

Here, we investigated our hypothesis that apoptotic dying cells produce growth-stimulating signals to induce an overproliferation of surviving neighboring cells. Our findings demonstrated a critical role of apoptotic SMC-derived PLF-1 in neointimal hyperplasia after acute injury. We also unexpectedly discovered that the ability of CatK to regulate TLR2-dependent caspase-8 maturation in the “execution” phase of cellular apoptosis is required for PLF-1-mediated growth-signaling pathway activation generated from the dying cells of an injured artery. We believe that this newly discovered PLF-1–mediated overgrowth mechanism may have key roles in wound healing, regeneration, and tumor repopulation.

Methods

The authors declare that all supporting data are available within the article.

Animals

Male wild-type (CatK^{+/+}) and CatK-deficient (CatK^{-/-})⁴ mice were 8 weeks old and weighed 21 to 24 g used for the ligation (n=39 for each group) and ligation plus cuff-replacement (n=42 for each group) injuries. In addition, male Wistar rats (3–4 months old; Japan SLC, Hamamatsu, Japan;

n=43) were used in the balloon injury study. Animal protocols were approved by the Institutional Animal Care and Use Committee of Nagoya University (Protocol No. 29392) and performed according to the *Guide for the Care and Use of Laboratory Animals* published by the National Institutes of Health.

Animal Studies and Tissue Collections

Rats were anesthetized with an intraperitoneal injection of pentobarbital sodium (50 mg/kg; Daiippon Pharmaceutical, Osaka, Japan), and a balloon catheter injury model to the rat

left common carotid artery was performed as described.¹⁶ In mice, the right common carotid artery was ligated just proximal to its bifurcations as described (single injury)³⁰; a polyethylene cuff (outside diameter 0.965 mm, inside diameter 0.580 mm, length 2 mm; Becton Dickinson, Lincoln Park, NY) was applied just proximal to the ligated site (double injury).³¹ For exploring molecular mechanisms, 3 independent experiments were conducted as follows: (1) Mice that had undergone the double injury were injected subcutaneously with saline (vehicle) or mouse rPLF-1 (recombinant PLF-1; 50 μ g/kg/day) on days -1, 1, 3, 5, and 7 postsurgery; (2) mice that had undergone the double injury were injected

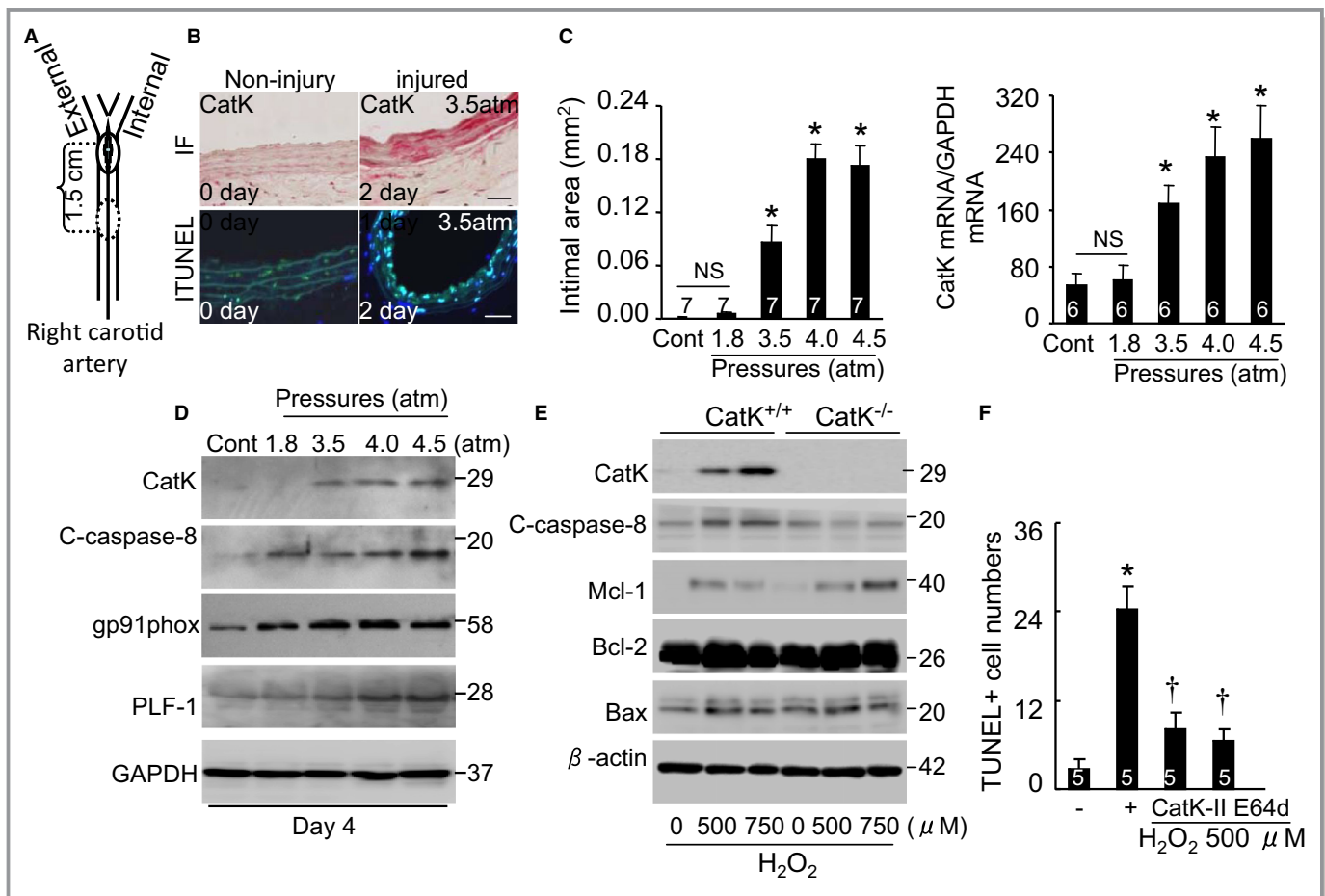


Figure 1. Injury produced cathepsin K (CatK) expression, apoptosis, and neointima hyperplasia. Schematic diagram of balloon-injury surgery in rat right carotid artery (A). Representative CatK and terminal deoxynucleotidyl transferase dUTP nick end labeling (TUNEL) staining images of rat carotid arteries at indicated days postsurgery (B). Scale bar, 50 μ m. Relative neointima areas in response to balloon pressure (n=7; C, left). Relative mRNA levels of CatK in response to balloon injury (n=7; C, right). Representative gel blots showing relative protein levels of CatK, caspase-8, gp91phox, and proliferin-1 (PLF-1) during exposure to balloon pressure (D). CatK^{+/+} and CatK^{-/-} smooth muscle cells (SMCs) were treated with or without H₂O₂ as used here for 24 hours, and then the culture media were collected for western blotting assays. Representative gel blots showing relative protein levels of CatK, Mcl-1, Bcl-2, and Bax during H₂O₂ exposure (0–750 μ M/L; E). CatK^{+/+} SMCs were treated with H₂O₂ in the presence or absence of either the CatK-specific inhibitor CatK-II (10 μ M/L) or the nonspecific cathepsin inhibitor, E64d (20 μ M/L), for 24 hours and then subjected to TUNEL staining for the analysis of cell apoptosis (n=5; F). Data are means \pm SEM. **P*<0.01 (vs the corresponding controls); †*P*<0.001 (vs H₂O₂ alone); NS, not significant by one-way ANOVA and Tukey's post hoc tests. Bax indicates Bcl-2-associated X protein; Bcl-2, B-cell lymphoma 2; Mcl-1, myeloid cell leukemia sequence 1; PLF-1, proliferin-1.

subcutaneously with either control mouse immunoglobulin G (IgG) or neutralizing mouse monoclonal antibody against (N-mAb-P, 150 µg/kg/day; R&D Systems, Minneapolis, MN) as indicated time points; and (3) injured mice were also injected subcutaneously with either DMSO or a synthetic caspase-8 inhibitor Z-IETD-FMK (Ze-I-E[OMe]-T-D[OMe]-FMK (5 mg/kg/day, FMK007; R&D Systems) as indicated.

At the indicated time points postsurgery, animals were euthanized with an overdose of sodium pentobarbital. For biological evaluation, animals were perfused with isotonic saline at physiological pressure, and then the arteries were isolated and kept in RNAlater solution or liquid nitrogen. For morphological studies, after being immersed in fixative with 4% PFA phosphate buffer solution for 16 hours (4°C), vessels were embedded in Tissue Tek optimal cutting temperature compound (Sakura Finetek, Tokyo, Japan) and stored at -30°C.

Morphometric and Immunohistological Analyses

In rats, 5-µm-thick cryosections at different parts (proximal, middle, and distal) of the carotid arteries segments were prepared. Cross-cryosections (5 µm) of the mouse carotid arteries were prepared at 2 mm proximal to the ligated site. Corresponding sections were stained with hematoxylin and eosin. Perimeters of the lumen, the external elastic lamina and the internal elastic lamina, were obtained by tracing the contours on digitized images. We measured the neointimal area by subtracting the lumen area from the area fixed by the internal elastic lamina, and we calculated the medial area by subtracting the area fixed by the internal elastic lamina from the area fixed by the external elastic lamina. In all immunohistological and morphometric analyses, 6 cross-sections (2 sections each from the proximal, middle, and distal regions) of vessels in each artery were measured for internal elastin length, media, and neointima, and then the results were averaged as described.^{4,16}

Carotid arterial slices on separate slides were processed for immunohistochemical analysis of CatK, PLF, Mac3 (macrophage-3), CD31, and α-SMA (α-smooth muscle actin). Primary antibodies for CD31 (1:50; ab28364; Abcam, Cambridge, MA), α-SMA (1:100; Clone 1A4; Sigma-Aldrich, St. Louis, MO), Mac3 (1:200; Clone M3/84; BD Pharmingen, San Diego, CA), and PLF (1:100; AF1623 to mouse tissues; R&D Systems) were applied to the sections, which were then left overnight at 4°C. After being washed with PBS 3 times, sections were sequentially treated with appropriate secondary antibodies (1:200–250; all from Vector Laboratories, Burlingame, CA), respectively, for 1 hour at room temperature, and were then visualized with a corresponding substrate kit (Vector Laboratories).

Terminal deoxynucleotidyl transferase dUTP nick end labeling and Bromodeoxyuridine Assays and Immunofluorescence Analysis

A terminal deoxynucleotidyl transferase dUTP nick end labeling (TUNEL) assay was conducted using the In Situ Cell Death detection kit, according to the manufacturer's instructions (Roche, Mannheim, Germany). In vivo bromodeoxyuridine (BrdU) labeling was conducted to determine the number of proliferating cells in injured arteries by detection of DNA synthesis using the BrdU immunohistochemistry kit (ab125306; Abcam). An intraperitoneal injection of BrdU (BD Pharmingen) was administered to mice at 100 µg/g body weight. Two hours later, carotid arteries were isolated and fixed in 4% PFA at 4°C overnight and then were imbedded in optimal cutting temperature compound (Sakura Finetek); serial sections were then collected for BrdU staining. Tissues for immunofluorescent BrdU staining were obtained after fixation in 4% PFA at 4°C for overnight and embedded in optimal cutting temperature compound. Then, 5-µm-thick cryosections on slide glass were applied for immunofluorescence staining.

Tissues for other immunofluorescence analyses from rat and mouse tissues were harvested after fixation after overnight 4% PFA fixation at 4°C. Tissues slices (5-µm) were processed for immunostaining of PLF-1 and α-SMA. Primary antibodies for PLF-1 (1:50; AF1623; R&D Systems) and α-SMA (1:100; NeoMarker, Fremont, CA) were loaded to tissue slices overnight at 4°C. After being washed with PBS 5 times, tissue slices were sequentially incubated with appropriate FITC- and PE- or Alexa-conjugated

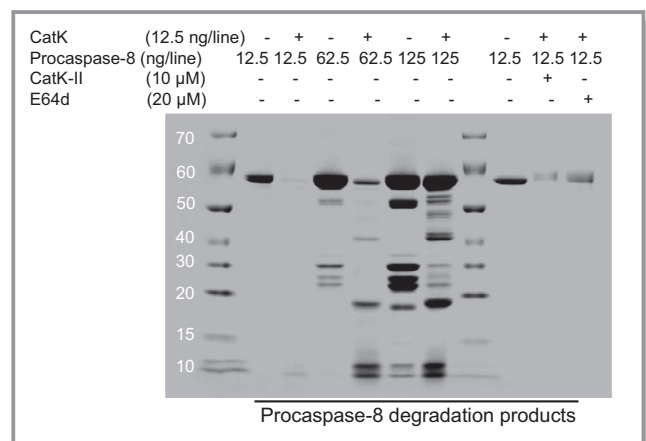


Figure 2. Recombinant human CatK (rhCatK)-mediated degradation of recombinant human procaspase-8. Precursor form of caspase 8 was incubated with rhCatK at the indicated concentrations, respectively, in buffer containing 50 mmol/L of sodium acetate, pH 6.8, 2.5 mmol/L of EDTA, 0.01% Triton X-100, and 1 mmol/L of DTT for 6 hours. Results were loaded to SDS-PAGE, and gels were then stained with CBB for visualization of procaspase degradation. Representative images show rhCatK-mediated procaspase-8 degradation. CatK indicates cathepsin K.

secondary antibodies (Invitrogen, Carlsbad, CA) for 1 hour. Staining sections were visualized with a BZ-X700 microscope (Keyence, Osaka, Japan) using $\times 20$ or $\times 40$ objectives. Images were analyzed with BZ-X analyzer software (Keyence).

Gene Expression Assay

RNA was harvested from tissue with an RNeasy Fibrous Tissue Mini-Kit and from cultured cells with an RNeasy Micro Kit (Qiagen, Hilden, Germany) in accord with the manufacturer's instructions. mRNA was reverse-transcribed to cDNA with an RNA PCR Core kit (Applied Biosystems, Foster City, CA). Quantitative gene expression was studied using the ABI 7300 real-time PCR system with Universal PCR Master Mix (Applied Biosystems). All experiments were performed in triplicate.

Gene expression assay IDs for mouse M6PR, PLF-1, and IGF2R (insulin-like growth factor 2 receptor) were as Mn04208409-9H, Mn04208104-9H, and Mn00439576-m1. Transcription of targeted genes was normalized to GAPDH (5'-AGGTGGTCTCCTGTGACTTC-3' and 5'-CTGTTGCTGTAGCCA AATTCG-3'). Conventional PCR was also performed for several targeted gene expressions, with the following conditions: 95°C for 20 seconds followed by 40 cycles at 95°C for 5 seconds and 55°C for 27 seconds, followed 95°C for 15 seconds and 60°C for 15 seconds.

Western Blot Analysis

Proteins were lysed from cells and tissues using lysis buffer containing 20 mmol/L of Tris-Cl (pH 8.0), 1% Triton X-100,

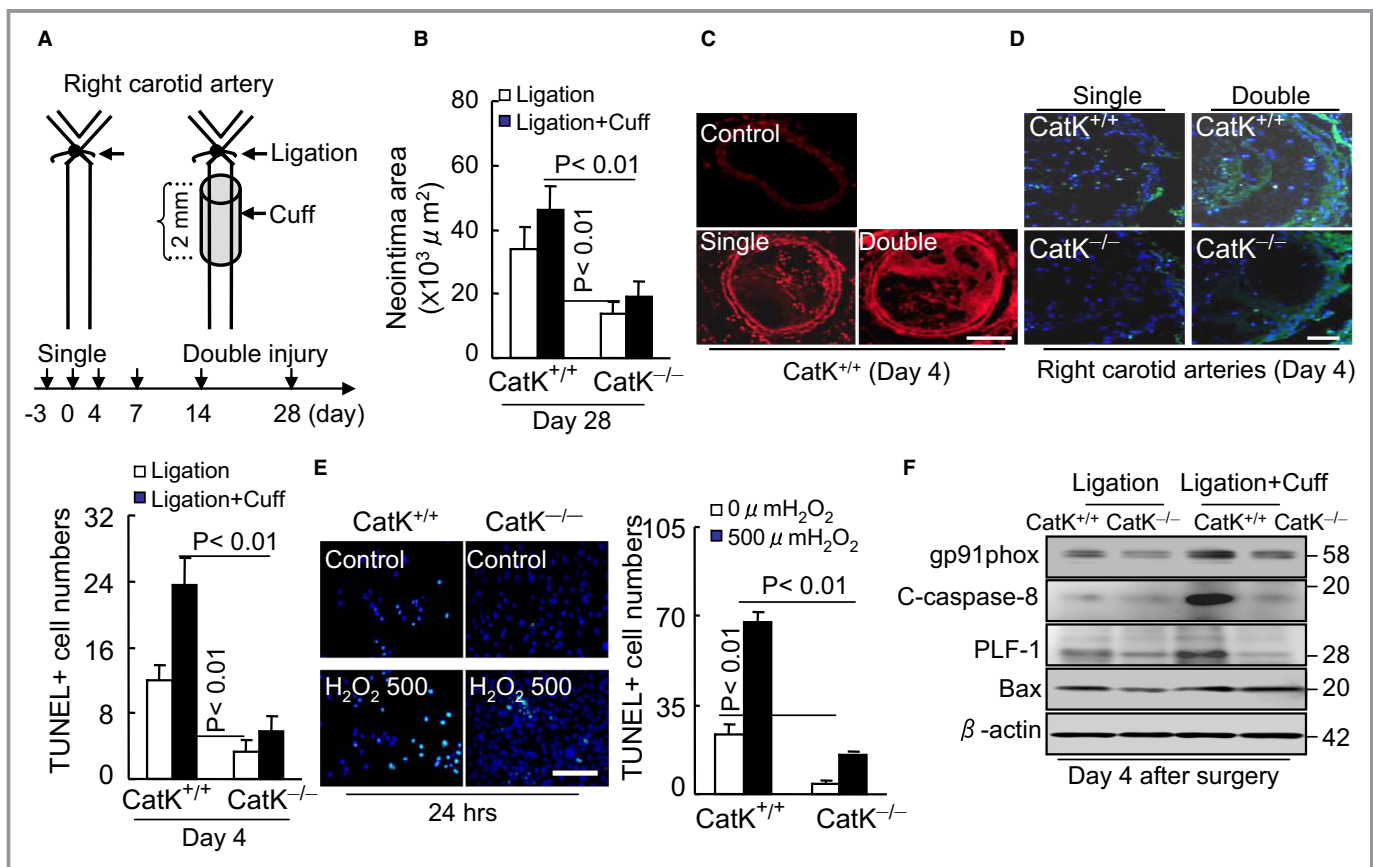


Figure 3. CatK silencing ameliorated vascular repair in response to injuries. Schematic diagram of single and double injuries in mouse right carotid artery (A). On day 28 postsurgery, left and right carotid arteries of CatK^{+/+} and CatK^{-/-} mice that had received a single or double injury were collected and subjected to H&E staining for quantitative analysis of the neointima areas in the 4 experimental groups (n=7–9; B). Representative dihydroethidium staining show superoxide production in injured arterial tissues of CatK^{+/+} mice (C). Representative TUNEL staining images and quantitative data showing TUNEL⁺ cells in injured (single and double) arterial tissues CatK^{+/+} and CatK^{-/-} mice in 2 experimental groups of (n=6; D). Scale bar, 50 μm. CatK^{+/+} and CatK^{-/-} SMCs were treated with or without H₂O₂ (500 μmol/L) for 24 hours and then subjected to TUNEL staining (n=7). Representative images of TUNEL staining (green) and combined quantitative data for TUNEL⁺ cells (gray/DAPI blue; E). Representative gel blot exhibiting the reduction of gp91phox, cleaved caspase-8, and PLF proteins, but not Bax protein, in injured arteries of CatK^{-/-} mice that received a single or double injury (F). Data are means±SEM. P values were calculated using Tukey's post hoc tests. Bax, Bcl-2-associated X protein; CatK, cathepsin K; DAPI, 4',6-diamidino-2-phenylindole; PLF-1, proliferin-1; SMCs, smooth muscle cells; TUNEL, terminal deoxynucleotidyl transferase dUTP nick end labeling.

150 mmol/L of NaCl, 1 mmol/L of EDTA, 0.05% SDS, 1% Na-deoxycholate, and fresh $1\times$ proteinase inhibitor. The concentration of each protein was measured by the DC protein assay kit (Bio-Rad Laboratories, Hercules, CA) before the proteins were equally loaded and separated by SDS-PAGE. Proteins were then transferred to Pall Fluorotrans-W membranes and incubated overnight with primary antibodies against Akt (protein kinase B; 2967), pAkt^{s473} (4060), pmTOR^{s2448} (2971), mTOR (mammalian target of rapamycin; 4517), GSK3 α/β (glycogen synthase kinases α and β ; 5676), pGSK3 α/β ^{s21/9} (9331), peEF2^{t56} (2331), eEF2 (eukaryotic elongation factor 2; 2332) pp38MAPK^{t180/t182} (4511), p38MAPK (9212), pERK^{t202/t204} (4377), ERK1/2 (9107), caspase-8 (4927), Bcl-2 (B-cell lymphoma 2; 2870), Bax (Bcl-2-associated X protein; 2772), (Mcl-1; 5453), Bcl-xL (B-cell lymphoma-extra large; 2764), cleaved caspase-9 (9509, 1:1000; Cell Signaling Technology, Danvers, MA), β -actin (AC-15, 1:1000; Sigma-Aldrich), gp91phox (clone: 53), PLF (AF1623, 1:1000; R&D Systems), CatK (sc-49353), PLF (AF1623), PLF (sc-271891), and GAPDH (sc-20357, 1:500; Santa Cruz Biotechnology). Membranes were then treated with the HRP-conjugated secondary antibody at a 1:10 000 to 15 000 dilution. The Amersham ECL Prime Western Blotting Detection kit (GE Healthcare, Freiburg, Germany) was used for determination of targeted proteins. Protein levels quantitated from western blots were normalized by loading internal controls.

Construction of the Proliferin Expression Plasmids

For the construction of the C-terminal Flag-tagged proliferin expression plasmids, we used PCR to generate full-length mPLF-1 cDNA from a mouse SMCs cDNA library lacking the stop codon. The PCR fragment was in-frame subcloned into the *EcoRI* and *XhoI* restriction sites of pcDNA3.1-Flag and pcDNA3.1-GFP vectors. The integrity of the construct was then verified by sequencing.

Production and Purification of Mouse Recombinant PLF-1

The FreeStyle MAX CHO Expression System (Invitrogen) was used to generate rPLF. Briefly, FreeStyle Chinese hamster ovary (CHO) cells were cultured in FreeStyle CHO Expression Medium containing 8 mmol/L of L-glutamine and $0.5\times$ Pen-Strep and incubated in a 37°C incubator containing a humidified atmosphere of 8% CO₂ in air with shaking at 120 rpm/min. Log-phase FreeStyle CHO cells ($\approx 1\text{--}1.5\times 10^6$ cells/mL density) were diluted into fresh FreeStyle CHO Expression Medium at 1×10^6 /mL and then subjected to the transfection procedure. For the transfection procedure, 37.5 μ L of FreeStyle MAX reagent was diluted with 0.6 mL of

OptiPRO SFM, and 37.5 μ g of pcDNA3.1-PLF-Flag plasmid was diluted into 0.6 mL of OptiPRO SFM. The diluted FreeStyle MAX Transfection Reagent was then mixed with the diluted DNA solution and incubated for 10 minutes at room temperature. The DNA-FreeStyle MAX Reagent complex was mixed with the CHO cells in a flask (total cell, 1×10^7 /30 mL), and mPLF-1 protein expression levels were monitored by performing a western blotting assay as indicated. On day 3 of transfection, media were collected by centrifugation at 250g for 5 minutes and stored at -70°C . rPLF purification and lyophilization were performed by Invitrogen (Life Technologies, Carlsbad, CA).

Proliferation and Apoptosis Assays

Approximately 2 to 3×10^3 cells were seeded in a 96-well plate, allowed to adhere overnight, and then incubated with fresh serum-free DMEM, PDGF-BB (50 ng/mL), or 2% FBS, rPLF-1, or additional drugs as indicated. After 48 hours, the number of cells was evaluated using a CellTiter 96 Aqueous nonradioactive cell proliferation assay kit (Promega, Madison, WI) according to the recommended protocol.⁴ Approximately 8 to 12×10^3 cells were plated in a 4-chamber polystyrene vessel tissue culture-treated slide (Falcon, Big Flats, NY), allowed to adhere overnight, and then cultured with either serum-free DMEM or conditioned media containing H₂O₂ or other drugs as indicated. After 24 hours, numbers of apoptotic cells were counted in 3 randomly selected fields of the slide using an In Situ Cell Death detection kit according to the manufacturer's instructions (Roche).

Cell-Cycle Analysis

A cell-cycle analysis was performed as described with minor modification.³² In brief, ≈ 2.0 to 2.5×10^5 cells were plated in a 6-well plate, allowed to adhere overnight, and then cultured with the stimulators as indicated. After trypsinization and centrifugation, cell pellets were suspended and fixed in 70% ethanol at 4°C overnight. Cells were sequentially incubated in KRISHIAN buffer (0.1% sodium citrate, 0.3% NP-40, 0.02 mg/mL of RNase A [Sigma-Aldrich], and 0.05 mg/mL of propidium iodide [Invitrogen]) for 1 hour at 4°C in the dark, and then filtered and evaluated for the propidium iodide labeling of DNA by flow cytometry.

Antibody Arrays

Apoptosis- and angiogenesis-related proteins of mouse and human SMCs, in aorta-derived SMCs treated with and without H₂O₂ in serum-free DMEM for 24 hours, were determined using the Proteome Profiler Human Apoptosis Array and

Mouse Angiogenesis Array kits (R&D Systems, ARY015 and ARY009; detecting 89 proteins), according to the recommended protocol. In brief, after conditioning media were harvested, cells were lysed with lysis buffer17 (895943), lysates were centrifuged for 30 minutes at 12 000g, and supernatants were collected. Protein levels of supernatants and condition media were assayed using the DC protein assay Kit (Bio-Rad Laboratories). Protein (160 μ g) was hybridized on the antibodies array overnight at 4°C. HRP-labeled streptavidin at 1:5000 dilution was used for the detection. Membranes were scanned using an LAS4010 imaging system and analyzed using ImageQuant TL software (GE Healthcare Japan, Tokyo). Results were then normalized using internal controls, and relative protein levels from 2 biological replicates are provided.

Pro-Caspase Degradation Assay

Precursor forms of caspase-8 and caspase-3 (both, R&D Systems) were incubated with recombinant human CatK (R&D Systems) in buffer containing 50 mmol/L of sodium acetate (pH 6.8), 2.5 mmol/L of EDTA, 0.01% Triton X-100, and 1 mmol/L of DTT for 24 hours. Results were loaded to SDS-

PAGE, and gels were then stained with Coomassie Brilliant Blue for visualization of pro-caspase degradation.

siRNA Transfection Protocol

Specific siRNAs against M6PR (Mm_m6pr_3685-s, Mm_m6pr_3685-as), IGF2R (Mm_igf2r8786_s, Mm_igf2r8786_as, Mm_igf2r4975_s, Mm_igf2r4975_as), TLR2 (Mm_Tlr2_5214_s and Mm_Tlr2_5214_as), caspase-3 (Mm_Casp3_0022_s and Mm_Casp3_0022_as), caspase-8 (Mm_Casp8_3293_s and Mm_Casp8_3293_as), and nontargeting control siRNA (Mission_SIC-001_s and Mission_SIC-001_as as the negative control) were purchased from Sigma-Aldrich. SMCs were grown on 60-mm dishes until 50% confluence. The siRNA solution mixed with serum-free and antibiotic-free DMEM-2 medium containing Lipofectamine RNAiMAX reagent (Invitrogen) was supplied to each well to achieve a final siRNA concentration of 100 pmol/L. Cells were treated at 37°C for 48 hours, and levels of targeted gene were analyzed by PCR.³³ Transfected cells were also used for cell proliferation experiments. Silamin A/C (D0010500105; Dharmacon, Brébières, France) was used as a positive control.

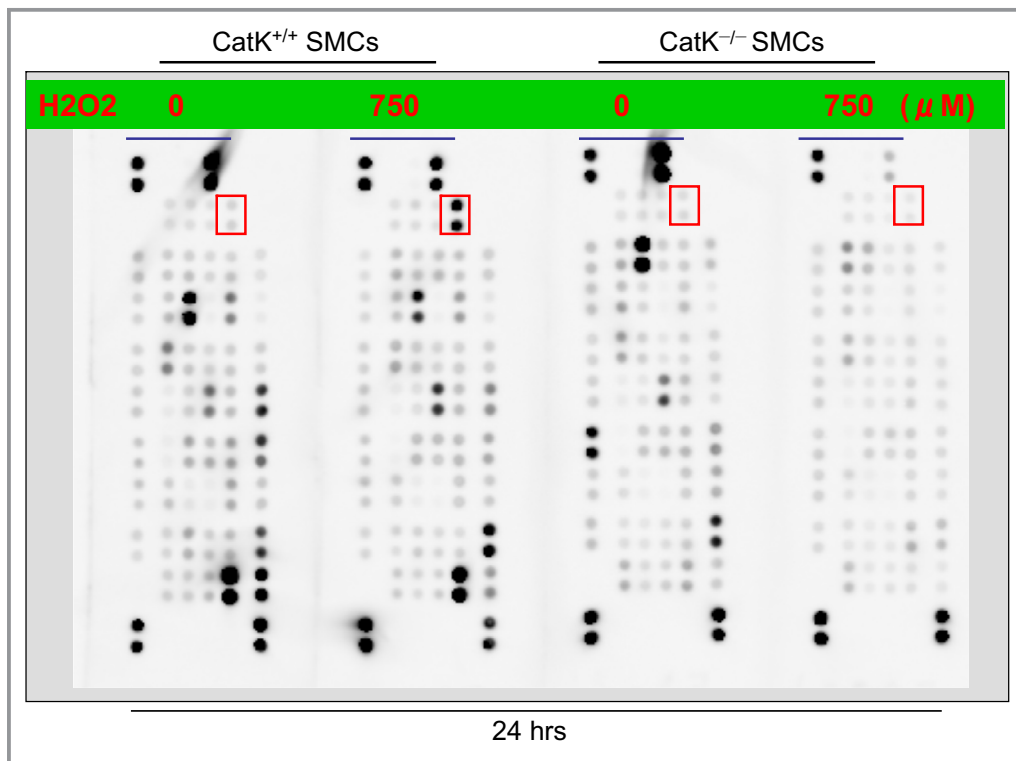


Figure 4. Comparison of the growth factor inductions between CatK^{+/+} and CatK^{-/-} SMCs in response to apoptotic oxidative stress. Following culturing in serum-free DMEM in the presence or absence of H₂O₂ (750 μ mol/L) for 24 hours, CatK^{+/+} and CatK^{-/-} SMC-conditioned media (total 160 μ g of protein) were subjected to a proteome profiler array. After hybridization and HRP labeling, membranes were scanned using an LAS4010 imaging system. CatK indicates cathepsin K; SMCs, smooth muscle cells.

Levels of PLF-1 Protein

At days 0, 4, 7, 14, and 28 postsurgery, levels of mouse plasma PLF-1 were determined using an ELISA kit developed by our laboratory. In this ELISA, PLF levels were determined using a standard curve generated with mouse rPLF short variant (PA-0659; Bioclone, San Diego, CA). Optimal absorbance density was calculated using a microplate reader (BioTex, Tokyo, Japan) at 450 and 600 nm. Mouse plasma PLF values are expressed as ng/mL, and the inter- and intra-assay coefficients of variation

were <8%. Each sample was measured in duplicate and averaged.

Statistical Analysis

Data are expressed as means±SE. Student *t* tests (for comparison between 2 groups) or 1-way ANOVA (for comparisons of ≥3 groups) followed by Tukey's post hoc tests were used for the statistical analyses. The nonparametric Kruskal–Wallis test (Tukey-type multiple comparison) was used for gene expression data. SPSS software (version 17.0;

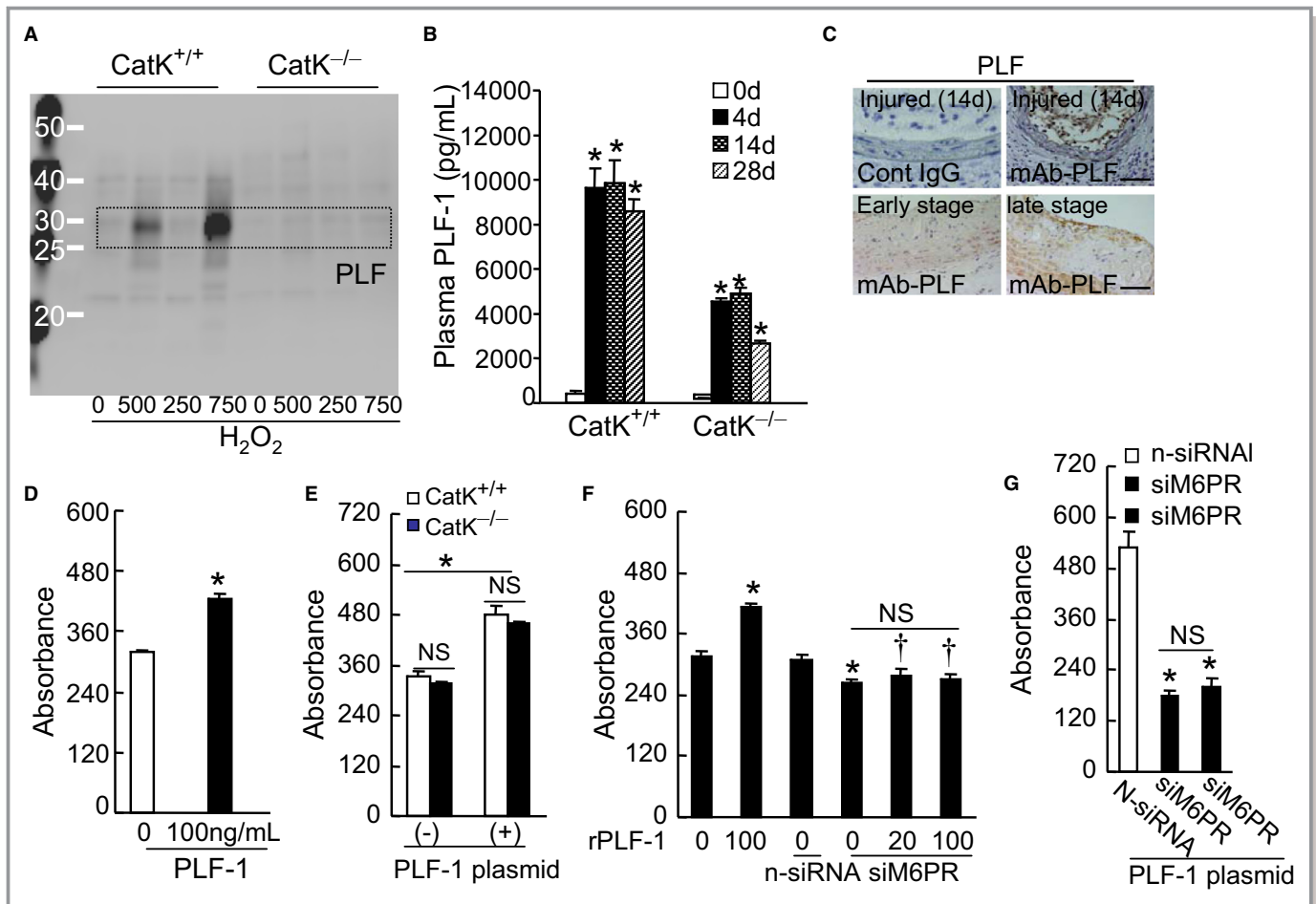


Figure 5. Apoptotic stress produced PLF in vitro and in vivo. Representative gel blots exhibiting the induction of PLF-1 protein during oxidative stress exposure (A). PLF-1 measured by ELISA in plasma of mice of both genotypes that had received the double injury (n=5–9; B). Expression of PLF-1 protein evaluated by immunostaining in plaques of CatK^{+/+} mice (C). Scale bar, 50 μm. CatK^{+/+} SMCs were incubated in the presence or absence of rPLF-1 for 48 hours and then subjected to a cell proliferation assay (n=6; D). CatK^{+/+} and CatK^{-/-} SMCs were transfected with empty vectors or mPLF-1 plasmid and then seeded onto 96-well plates and cultured in serum-free DMEM. After 48 hours, results were analyzed by cell proliferation assays (n=8; E). CatK^{+/+} SMCs were cultured in the presence or absence of nontargeted siRNA (n-siRNA) or short interfering mannose-6-phosphate receptor (siM6PR; 100 nmol/L for each). After 48 hours, cells were subjected to cell proliferation under rPLF-1 at the indicated times (n=5; F). Following treatment with n-siRNA and siM6PR for 2 days, cells were transfected again with mouse PLF-1 plasmid. After 48 hours, PLF-1-overexpressing cells were examined in a cell proliferation assay (n=8; G). Data are means±SEM. NS, not significant. **P*<0.01 (vs the corresponding controls); †*P*<0.001 (vs rPLF 100 ng/mL alone); NS, not significant by ANOVA and Tukey's post hoc tests. CatK indicates cathepsin K; PLF-1, proliferin-1; rPLF-1, recombinant proliferin-1; SMCs, smooth muscle cells.

SPSS, Inc, Chicago, IL) was used. A value of $P < 0.05$ was considered statistically significant.

Results

CatK Activation Is Required for Pro-Caspase-8 Maturation in SMC Apoptosis

As a first step to examine the relationship between apoptosis and CatK expression and activation in injury-related restenosis, we established a rat balloon-injury model (see Figure 1A). Consistent with a previous report,¹⁶ we observed only a low level of expression of CatK in the uninjured arterial tissues. In contrast, CatK expression was markedly increased throughout the media, with staining signaling apparent in SMCs on day 2 after the surgical injury (see Figure 1B, upper panels). Figure 1C illustrates the balloon pressure-dependent increase in neointimal hyperplasia accompanied by increased CatK expression. Similarly, the immunoblotting assay revealed that exposure to the balloon injury caused an enhancement of the active form of CatK protein (see Figure 1D). TUNEL staining showed that on day 2 postsurgery, there were extensive apoptotic cells in media of injured arteries compared with uninjured arteries (see Figure 1B, bottom panels). Moreover, levels of c-caspase-8 (cleaved caspase-8) protein, a key player in the apoptosis process, were markedly upregulated by surgical damage (see Figure 1D). Superoxide generation by NADPH oxidase has been shown to activate cathepsin.³⁴ gp91phox, which is 1 of the major NADPH oxidase components, is required for apoptosis in SMCs.³⁵ Here, we observed

that the injury-related stress enhanced gp91phox protein expression (see Figure 1D). Thus, CatK activation by oxidative stress appears to regulate caspase-8 maturation-mediated cell apoptosis in vascular tissues in response to surgical injury.³⁶

To further address the question of whether CatK contributes to pro-caspase-8 maturation, rhCatK (recombinant human CatK) was incubated with recombinant human pro-caspase-8 in the presence of several CatK inhibitors under an acidic experimental condition. Results indicated that pro-caspase-8 was sensitive to rhCatK, and this effect was inhibited by a specific CatK inhibitor (CatK-II) and a nonspecific cathepsin inhibitor (E64; see Figure 2). As shown in Figure 1E, CatK^{-/-} reduced levels of c-caspase-8 protein in response to H₂O₂ at the concentrations used. The parallel quantitative analysis of H₂O₂-induced apoptosis with TUNEL staining revealed that both CatK-II and E64d caused a decrease in SMC apoptosis to 67% and 77% less than that of cells treated with H₂O₂ alone (see Figure 1F), indicating that the ability of CatK to cleave pro-caspase-8 is likely to trigger SMC apoptosis in response to oxidative stress. However, there were no differences in levels of Mcl-1, Bcl-2, and Bax proteins between both groups (see Figure 1E).

CatK Deletion-Mediated Antiapoptosis Triggers Vascular Protective Action

We created carotid artery injury models (a single-injury model: ligation; and a double injury model: ligation plus polyethylene cuff replacement) using CatK^{+/+} and CatK^{-/-} mice

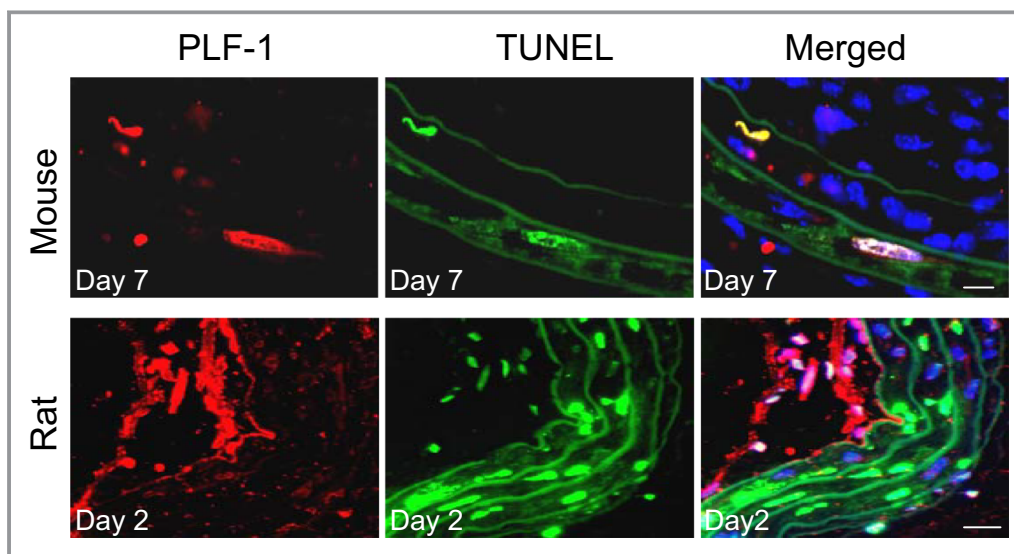


Figure 6. Apoptotic dying cells produced PLF in vivo. Representative double immunofluorescence images show apoptotic dying cell-derived PLF-1 in arterial lesions of mice that received the combination injury and rats that received a balloon injury. Scale bars, 100 μ m. PLF-1 indicates proliferin-1; TUNEL, terminal deoxynucleotidyl transferase dUTP nick end labeling.

(see Figure 3A) to monitor the vascular biological and morphological actions. Consistent with a previous study,⁴ we observed marked intimal hyperplasia in $CatK^{+/+}$ mice on day 28 after the double injury and to a lesser extent after the single injury, and these changes were mitigated by $CatK$ deletion (see Figure 3B). Dihydroethidium staining showed a marked staining signal in the injured arterial tissues by both the single and double injuries of $CatK^{+/+}$ mice (see Figure 3C), indicating that the injuries accelerated oxidative stress production in the arteries. A quantitative analysis of TUNEL staining revealed that $CatK$ deficiency ameliorated medial SMC apoptosis in both injury models (see Figure 3D). Likewise, $CatK^{-/-}$ SMCs were resistant to H_2O_2 treatment at 500 $\mu\text{mol/L}$ (see Figure 3E). As shown in see Figure 3F, protein levels of gp91phox and the c-caspase-8 in injured arteries of $CatK^{-/-}$ mice were lower than in those of $CatK^{+/+}$ mice, suggesting that inhibition of caspase-8-related SMC apoptosis by $CatK$ deficiency could represent a common mechanism in the protection of vascular tissue to injury. However, there were no significant differences in levels of Bax

protein in the single- or double-injured arterial tissues between the 2 mouse genotypes. We recently reported that $CatK$ silencing confers vascular protective action against injury by reduction of SMC proliferation.⁴ This past finding raises the question of how $CatK$ deficiency and alteration of the apoptotic ability change intracellular signaling toward a reduction of the neighboring SMCs' proliferative action under the experimental conditions used here.

CatK^{-/-} Reduced the Interaction Between Apoptosis and Proliferation

Neointimal hyperplasia, an important feature of injury-related vascular remodeling and restenosis, depends on vascular cell apoptosis and proliferation. The communication between apoptosis and proliferation in the restenosis process has been unclear. Radiotherapy- and chemotherapy-induced dying cells have been shown to produce several growth factors that contribute to tumor repopulation,⁷ leading us to speculate that $CatK$ activation-related apoptotic dying cells could

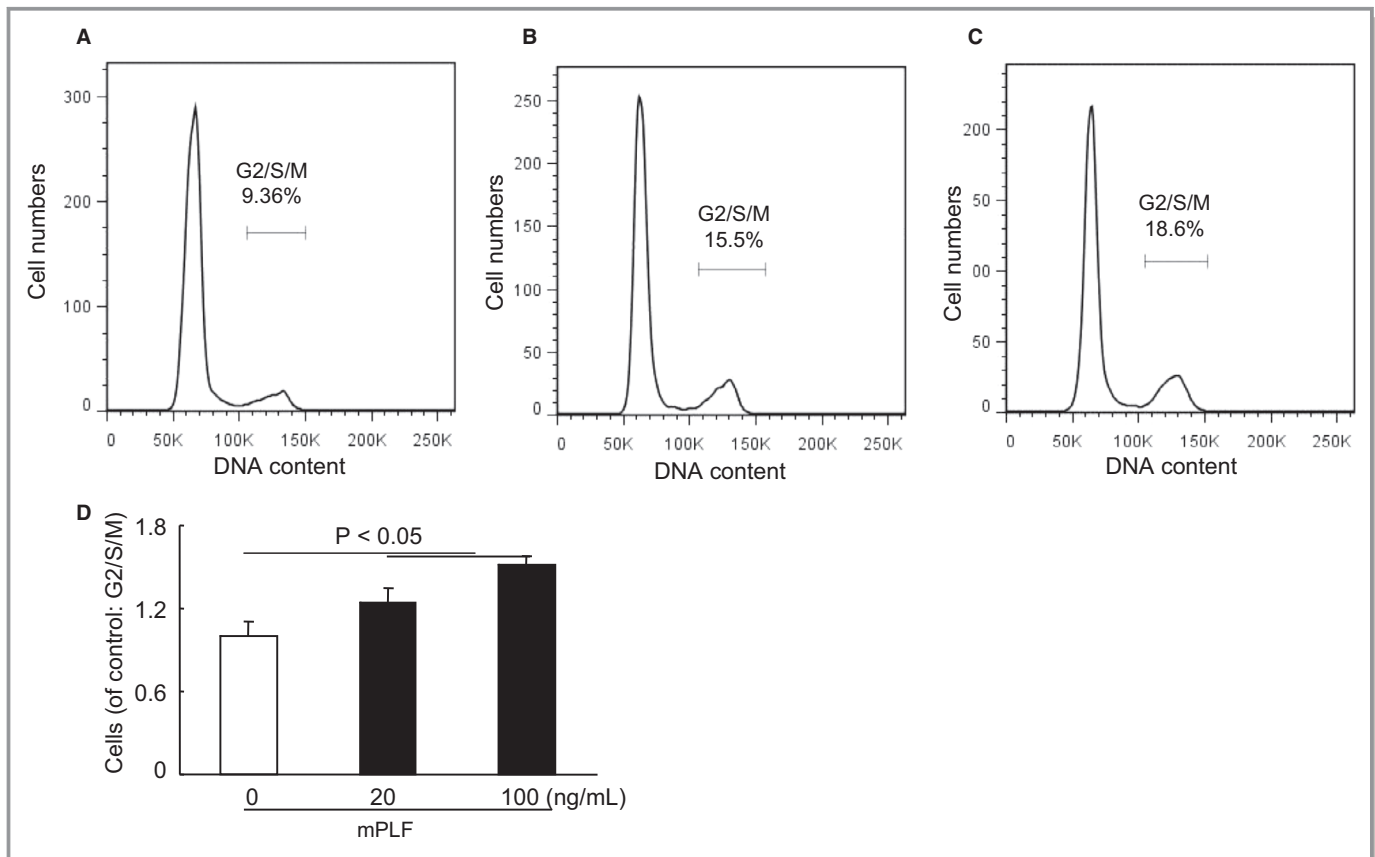


Figure 7. PLF-1 activates cell cycle. Mouse SMCs were plated in 6-well plates (2.5×10^5 /well), allowed to adhere overnight, and then incubated in the presence or absence of rPLF-1 at 20 and 100 ng/mL for 24 hours. After trypsinization and centrifugation, cell pellets were suspended and fixed in 70% ethanol at 4°C overnight and then evaluated for propidium iodide labeling of DNA by flow cytometry. Representative histograms of DNA content during the cell cycle (A through C). Distribution of cells in G2/S/M expressed as a percentage of total cells (n=7; D). PLF-1 indicates proliferin-1; rPLF-1, recombinant proliferin-1; SMCs, smooth muscle cells.

produce growth-promoting signals to stimulate the proliferation of surviving cells. To examine this hypothesis, we used a proteome profiler array to screen the changes of various growth factors in conditioned media of CatK^{+/+} and CatK^{-/-} SMCs treated with and without 750 $\mu\text{mol/L}$ of H₂O₂. As expected, among the 54 targeted factors, apoptotic stress increased levels of PLF (which is known as an angiogenic growth hormone) in CatK^{+/+} SMC-conditioned media. This effect was dramatically decreased by CatK deficiency (see Figure 4). The parallel immunoblotting analysis of the lysates showed that H₂O₂ treatment greatly increased levels of PLF protein in CatK^{+/+} SMCs, whereas it was not detected in CatK^{-/-} SMCs under our experimental conditions (see Figure 5A). Carotid artery injury experiments revealed that lesions of single- and double-injured arteries of CatK^{+/+} mice contained large amounts of PLF protein; these changes were less pronounced in both of the mouse models devoid of CatK (see Figure 3F). A previous study reported that oxidative stress can mediate PLF gene expression in tumor C3H10T1/2 cells.³⁷ CatK deletion thus appears to reduce oxidative stress-induced PLF-1 production and growth signal induction. Figure 1D presents a balloon pressure-dependent increase in PLF-1 protein expressions of injured rat carotid arteries. On the indicated operative days, TUNEL staining combined with immunofluorescence revealed that PLF-1 was localized in TUNEL⁺ cells of the neointima and media cells of mice and rats (see Figure 6), suggesting that apoptotic dying cells could produce PLF-1 to stimulate proliferation of surviving cells.

Plasma PLF-1 Was Increased by Vascular Injury in Animals

We observed that plasma PLF-1 levels had significantly increased as early as day 1 in both genotypes of mice and peaked at day 14 after the combination injury and remained at high levels for up to 28 days (see Figure 5B), implying that circulating PLF-1 could be a novel predictor of vascular injury in mice. Immunostaining showed that expression of PLF-1 was markedly increased throughout the intima and media of injured arteries (see Figure 5C). Additionally, CatK^{-/-} mice showed reduced plasma PLF-1 levels compared with corresponding control CatK^{+/+} mice (see Figure 5B), indicating that PLF reduction is likely to contribute to CatK ablation-mediated vascular benefits.

PLF-1/M6PR Was Required for SMC Proliferation

PLF is involved in endothelial cell proliferation, and blockade of PLF suppresses angiogenesis in several in vitro and in vivo models.^{29,38} As anticipated, PLF-1 stimulated CatK^{+/+} SMC proliferation (see Figure 5D). We used the gain-of-function approach to further test PLF-1's role in cell growth. PLF-1

overexpression resulted in enhanced proliferative abilities of SMCs of both genotypes (see Figure 5E). A propidium iodide cell-cycle analysis also revealed that PLF-1 caused an increase in the number of proliferating cells (G2/M/S) in a dose-dependent manner (see Figure 7). Additionally, because M6PR was reported as a major receptor of PLF involved in cellular functions,^{39,40} we tested a short interfering RNA against M6PR (siM6PR) in SMCs. CatK^{+/+} SMCs transfected with siM6PR showed dramatically decreased M6PR gene expression (see Figure 8) and exhibited no proliferative action in response to PLF-1 or PLF-1 plasmid intervention (see Figure 5F and 5G). PLF-1/M6PR thus appears to be required in SMC proliferation in response to injury.

PLF Regulates SMC Proliferation by PI3K/Akt/p38MAPK-Dependent and -Independent mTOR Signaling Activation

To study the intracellular mechanism by which PLF controls cell growth, a series of protein kinase activity assays with CatK^{+/+} SMCs and recombinant mouse PLF were performed in the presence of several specific protein kinase inhibitors. Expectedly, results indicated that PLF increased phosphorylation levels of Akt and mTOR in a dose-dependent manner (see Figure 9A). Likewise, PLF-1 also increased levels of p-Akt, p-p38MAPK, p-mTOR, p-GSK-3 α/β , and p-EF in a time-dependent manner (see Figure 9B). Moreover, we observed that except Erk 1/2 inhibitor U0124, PI3K inhibitor LY294002 and P38MAPK inhibitor 203580 exhibited inhibitory effects on the phosphorylations of Akt, mTOR, and p38MAPK, but not U0124 (see Figure 9C), leading us to speculate that upregulation of PI3K/Akt-p38MAPK-dependent and -independent

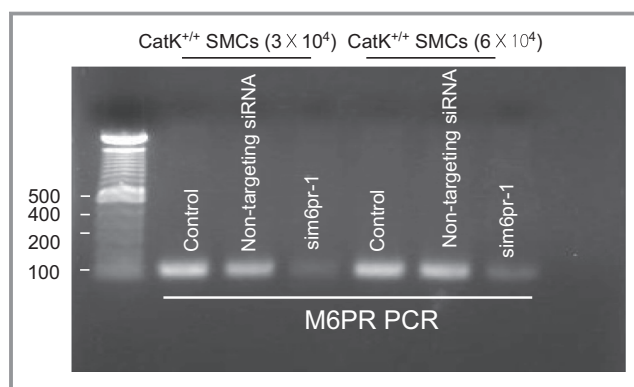


Figure 8. siM6PR suppressed its mRNA expression in SMCs. Mouse SMCs were seeded into 3-cm dishes at the density of 3×10^4 and 6×10^4 cells/well, then treated with either non-targeted siRNA or siM6PR at 100 nmol/L for 24 hours. RT-PCR was then used to determine the mRNA expression. CatK indicates cathepsin K; SMCs, smooth muscle cells.

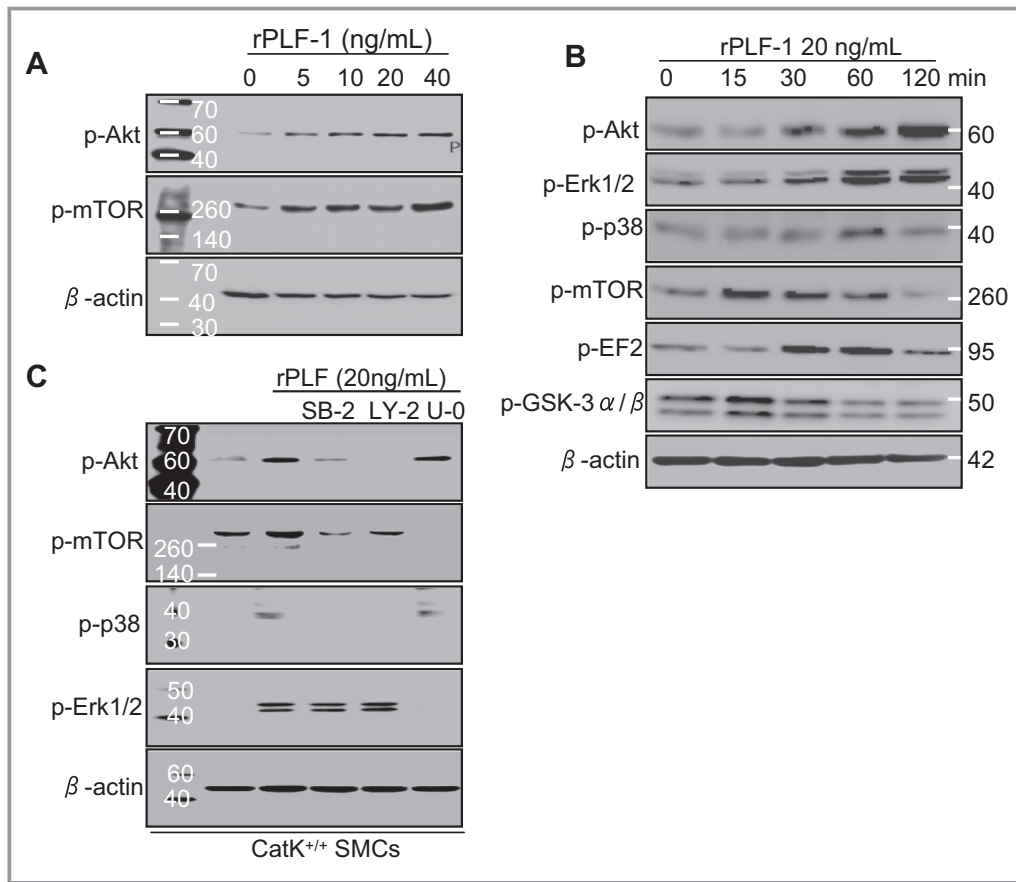


Figure 9. Mouse recombinant PLF-1 produced potent growth-stimulating signals. SMCs were seeded into 6-well plates and then treated with PLF-1 as indicated for 30 minutes. Representative immunoblots exhibit a dose-dependent change in levels of p-Akt and p-mTOR proteins (**A**). SMCs were treated with rPLF-1 for the indicated times. Related protein levels of p-Akt, p-Erk1/2, p-p38, p-mTOR, t-EF2, and p-GSK3 α/β during rPLF-1 exposure (15–120 minutes; **B**). Following pretreatment with a PI3K inhibitor (LY29002, LY), a p38 inhibitor (SB203580, SB), or an Erk1/2 inhibitor (U0124, U-0; 5 μ mol/L each) for 30 minutes, cells were subjected to the related intracellular signaling activation. Representative gel blots show the changes in levels of rPLF-1-induced p-Akt, p-mTOR, p-Erk1/2, and p-38 proteins during exposure to several signal kinase inhibitors (**C**). Akt indicates protein kinase B; CatK, cathepsin K; Erk1/2, extracellular signal-regulated kinases 1 and 2; GSK3 α/β , glycogen synthase kinases α and β ; mTOR, mammalian target of rapamycin; p-, phosphorylated; PI3K, phosphatidylinositol 3-kinase; PLF-1, proliferin-1; rPLF-1, recombinant proliferin-1; SMCs, smooth muscle cells; t-EF2, translation elongation factor 2.

cascade activation by PLF-1 is a molecular mechanism of SMCs' proliferation.

PLF-1 Blocking Mitigates Neointimal Hyperplasia

We began to investigate the ability of PLF-1–blocking antibody to modulate vascular remodeling in response to injury in CatK^{+/+} mice. On operative day 14, N-mAb-P administration significantly suppressed neointimal formation (see Figure 10A and 10B). PLF-1 blocking had a significant reduction in the number of BrdU⁺ proliferating cells in the neointima and media of the PLF-1–blocked group of mice (see Figure 10A and 10C). Likewise, N-mAb-P also reduced the ratio of BrdU⁺

proliferating cells to total neointimal cells and total medial cells (see Figure 10C). On operative day 4, the double immunofluorescence of injured artery sections with antibodies to the SMC- and proliferating cell–specific marker revealed that BrdU was localized in SMCs (see Figure 10D). Although PLF-1 blocking had no effects on superoxide production or gp91phox protein level (see Figure 10E), western blotting assays revealed that it suppressed levels of arterial tissue p-Akt, p-p38MAK, and p-mTOR proteins (see Figure 10F). These results thus indicated that PLF-1 deletion by a neutralizing antibody can modulate injury-related vascular repair by reduction of PI3K/Akt/mTOR signaling activation without oxidative stress production in mice.

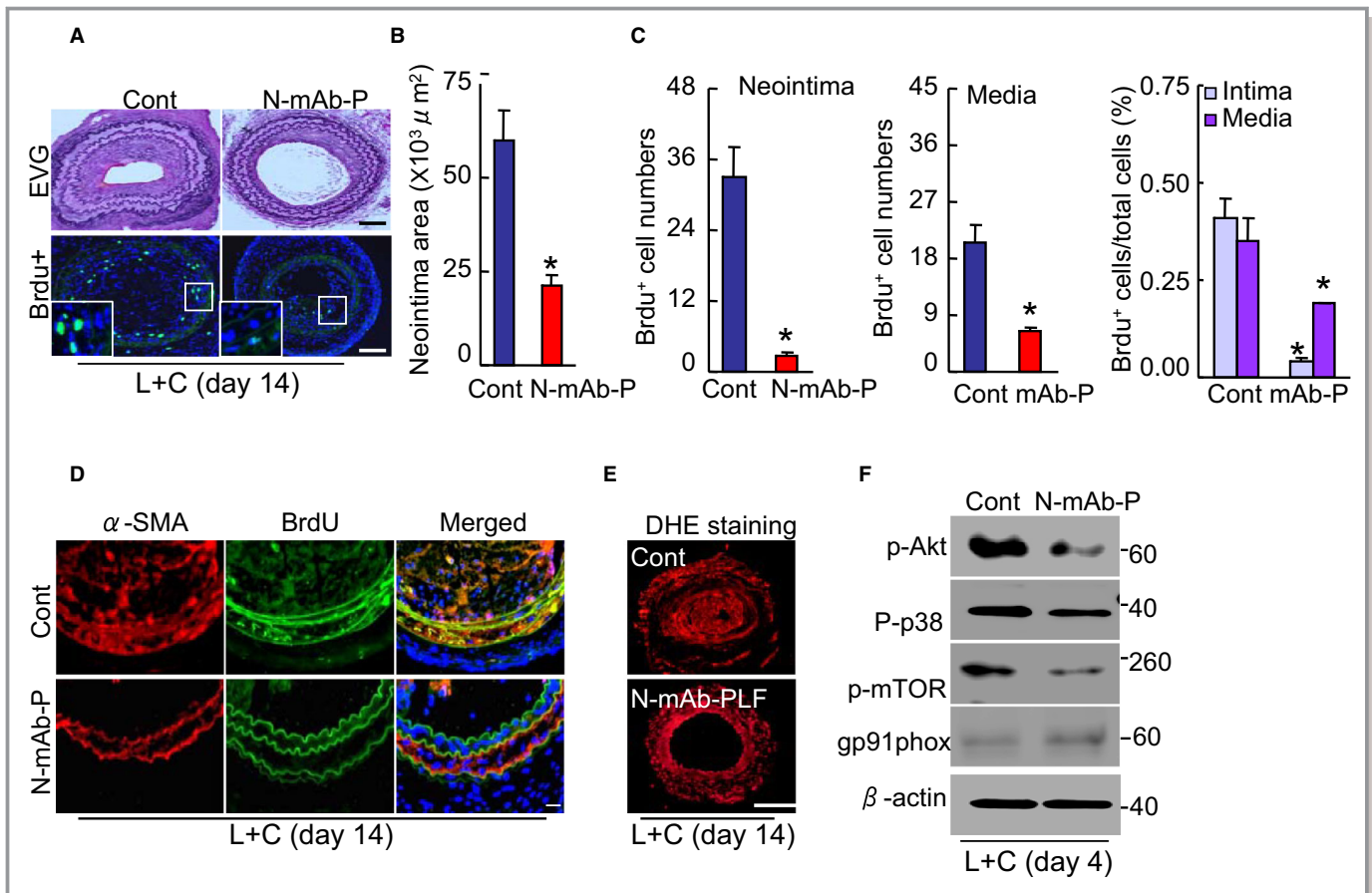


Figure 10. PLF depletion mitigated injury-related vascular actions in mice. $CatK^{+/+}$ mice that had undergone the double injury were injected subcutaneously with either control IgG (Cont) or neutralizing mAb against PLF (N-mAb-P; 150 μ g/kg/day for each) on days -1 , 1 , 3 , 5 , and 7 postsurgery. On operative day 14 , after an intraperitoneal injection of bromodeoxyuridine (BrdU; 100 μ g/kg) for 2 hours, carotid arteries were isolated for histological analysis. Representative H&E and BrdU staining images of injured arteries (**A**). Scale bar, 50 μ m. Quantitative data showing the neointima area, BrdU⁺ cells in neointima and media, and percentage of BrdU⁺ cells of total cells (neointima plus media) in injured arteries of the 2 experimental groups ($n=6$; **B** and **C**). Representative double BrdU/ α -SMA immunofluorescence image of neointima and media SMC proliferation (**D**). Representative dihydroethidium (DHE) staining showing superoxide production in injured arterial tissues (**E**). Representative gel blots exhibiting reductions of p-Akt, p-p38, and p-mTOR proteins, but not gp91phox, in injured arteries of N-mAb-P group mice (**F**). Data are means \pm SEM. * $P<0.01$ (vs corresponding controls); NS, not significant by ANOVA and Tukey's post hoc tests. Akt, protein kinase B; CatK, cathepsin K; EVG, Verhoeff-Van Gieson elastic staining; IgG, immunoglobulin G; mTOR, mammalian target of rapamycin; p-, phosphorylated; PLF, proliferin; α -SMA, alpha-smooth muscle actin; SMCs, smooth muscle cells; L+C, ligation+Cuff.

Recombinant PLF-1 Accelerates Neointimal Hyperplasia

We investigated the possibility that administration of mouse recombinant PLF-1 can modulate vascular remodeling in response to injury in $CatK^{+/+}$ mice. On day 14 postsurgery, PLF-1 administration enhanced the neointimal area and ratio of the neointima to media (see Figure 11A and 11B). Similarly, PLF-1 caused increases in not only the numbers of BrdU⁺ proliferating cells in both neointima and media, but also the ratio of BrdU⁺ proliferating cells to total neointimal and media cells (see Figure 11A and 11C).

CatK Triggers PLF-1 Expression by TLR2/Caspase-8-Dependent Mechanism

Finally, we investigated whether caspase-8 silencing or inhibition mitigates PLF-1 expression in vitro and in vivo. As shown in Figure 12A, siRNA-targeted caspase-8 (siCasp8) was able to reduce PLF-1 expression induced by H₂O₂ treatment. Data of our in vivo experiments showed that a synthetic specific caspase-8 inhibitor, Z-IETD-FMK, suppressed not only PLF-1 expression, but also levels of the cleaved caspase-8 proteins (43–18 kDa productions; see Figure 12B and 12C), suggesting that caspase-8 inhibition is also likely to contribute to reduction of PLF-1 production and

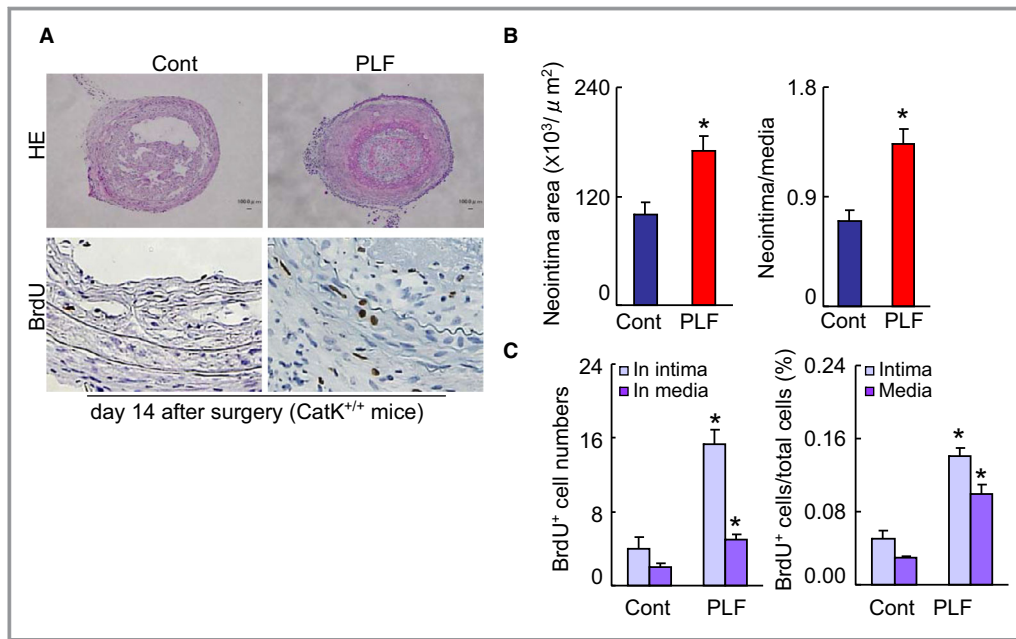


Figure 11. PLF-1 administration accelerated vascular remodeling in $\text{CatK}^{+/+}$ mice. $\text{CatK}^{+/+}$ mice that had undergone the single injury were injected subcutaneously with either control PBS (Cont) or mouse recombinant PLF (50 $\mu\text{g}/\text{kg}$ per day) on days -1 , 1 , 3 , 5 , and 7 postsurgery. On operative day 14 , after an intraperitoneal injection of bromodeoxyuridine (BrdU; 100 $\mu\text{g}/\text{kg}$) for 2 hours, carotid arteries were isolated for histological analysis. Representative H&E and BrdU staining images of injured arteries (**A**). Scale bar, 50 μm . Quantitative data showing the neointima area, ratio of neointima to media, BrdU⁺ cells in neointima and media, and percentage of BrdU⁺ cells of total cells (neointima plus media) in injured arteries of the 2 experimental groups ($n=6-8$; **B** and **C**). Data are means \pm SEM. * $P<0.01$ (vs the corresponding controls) by ANOVA and Tukey's post hoc tests. CatK indicates cathepsin K; PLF-1, proliferin-1.

secretion in vivo and in vitro. TLR2 has been shown to modulate the caspase-8-related apoptotic signaling pathway.^{22,23} Here, we have observed that TLR2 silencing exhibited an inhibitory effect on oxidative stress-induced pro-caspase-8 expression and PLF-1 protein in cultured SMCs (see Figure 12D and 12E). In the in vitro experiments, CatK deficiency resulted in markedly decreased levels of TLR2 protein in SMCs under an oxidative stress condition (see Figure 12F). Consistently, as compared with $\text{CatK}^{+/+}$ mice, $\text{CatK}^{-/-}$ mice had lower levels of TLR2 protein in the injured arterial tissues (see Figure 12G). Collectively, these findings indicate that modulation of TLR2-dependent caspase-8 expression and activation by inhibition of CatK activity could represent a common mechanism in regulation of PLF-1 production and secretion in vivo and in vitro.

Discussion

An early hypothesis by Qin et al⁴¹ noted that there might be an inextricable link between vascular cell death and overproliferation in atherogenesis. Over the last 5 years, the importance of apoptosis in tissue repopulation and regeneration has been revealed by a few tumor biological studies.^{7,42}

Although those investigations uncovered key mechanisms of tumor regrowth and repopulation after cytotoxic cancer therapy, their findings do not explain the initial driving events responsible for hyperproliferative cardiovascular actions after angioplasty. In the present study, we focused on the novel mechanism and molecular requirement necessary for the link between cell apoptosis and overproliferation in the injury-related vascular repair process. The major findings were as follows: (1) CatK triggers PLF-1 expression and secretion by TLR2-mediated caspase-8 activation under the conditions of oxidative apoptotic stress. (2) PLF-1 released from apoptotic dying cells is a key mediator of the interactive link between SMC apoptosis and proliferation, and it regulates cell proliferative behavior through a PI3K/Akt/p38MAPK-M6PR-dependent and -independent mTOR signaling pathway. Our findings demonstrated that CatK ablation can modulate vascular actions by reduction of PLF-1 production associated with resistance to apoptotic stress.

Caspase-8 has been best characterized as a cysteine protease that degrades specific substrates to transmit to apoptotic signals downstream of death receptors.^{43,44} During death receptor signaling, pro-caspase-8 is recruited to the death-inducing signaling complex, where oligomerization

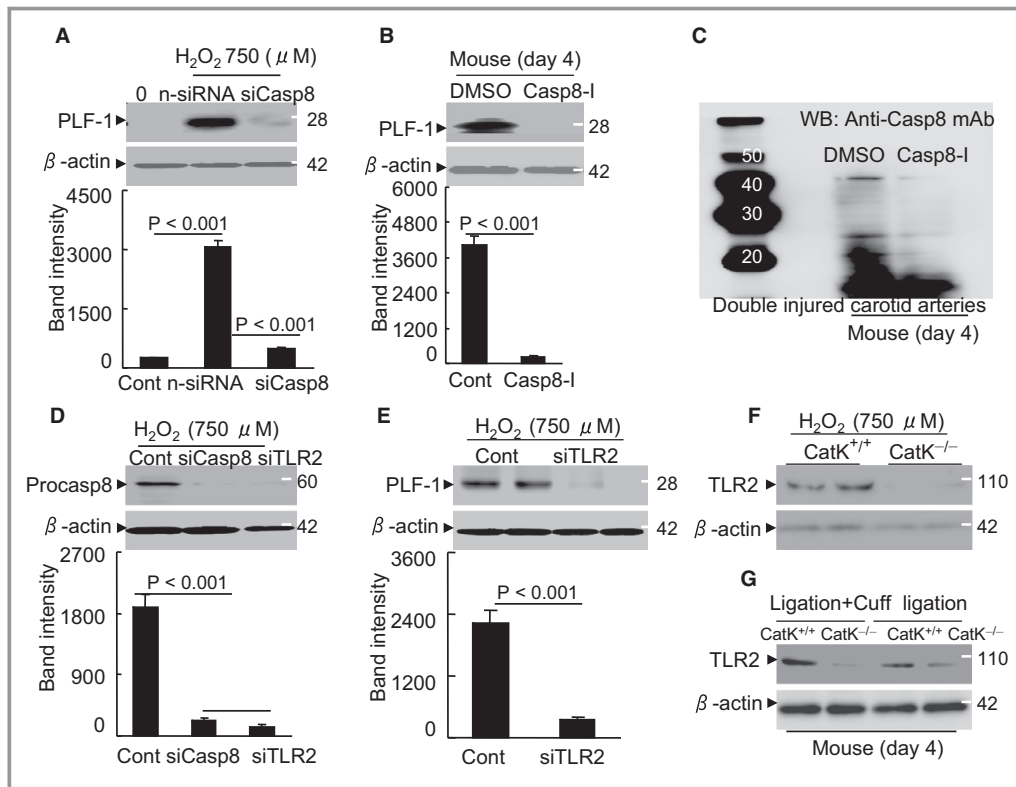


Figure 12. siCasp8 and caspase-8 inhibitor (Casp8-I) decreased PLF-1 expression in vitro and in vivo. SMCs were seeded into 6-well plates (2.5×10^5) and then treated with nontargeted siRNA (n-siRNA) or siCasp8, respectively, under H_2O_2 condition at indicated concentrations for 2 days. Lysates were subjected to western blotting assays. Representative immunoblots and quantitative data exhibit changes in levels of PLF-1 protein (A). $CatK^{+/+}$ mice that had undergone double injury were injected subcutaneously with either DMSO or a synthetic specific Casp8-I (5 mg/kg/day for each) on days -2, -1, 0, 1, 2, 3, and 4 postsurgery. On operative day 4, carotid arteries were isolated for western blotting. Representative images of western blots and quantitative show changes in levels of PLF-1 (B) and caspase-8 (C) proteins. SMCs were seeded into 6-well plates (2.5×10^5) and then treated with siCasp8 or siTLR2, respectively, at H_2O_2 condition for 2 days. Lysates were subjected western blotting assays. Representative immunoblots and quantitative data exhibit changes in levels of procaspase-8 (procasp8; D) and PLF-1 (E) protein. $CatK^{+/+}$ and $CatK^{-/-}$ SMCs were seeded into 6-well plates (2.5×10^5) and then treated with H_2O_2 (750 μ mol/L) for 24 hours. Lysates were subjected western blotting assays. Representative immunoblots and quantitative data exhibit changes in levels of PLF-1 protein (F). On operative day 4, left and right carotid arteries of $CatK^{+/+}$ and $CatK^{-/-}$ mice that had received a single or double injury were collected and subjected to western blotting assays. Representative immunoblots exhibit changes in levels of PLF-1 protein (G). Data are means \pm SEM ($n=3-5$ for each group). *P* values calculated using Student *t* test or Tukey's post hoc tests. CatK indicates cathepsin K; PLF-1, proliferin-1; SMCs, smooth muscle cells.

drives its own activation by self-cleavage to form an activated caspase-8 tetramer complex in a process termed "proximity-induced activation."⁴⁵ To the best of our knowledge, our observation is the first to show that CatK modulates pro-caspase-8 activation. We have shown that genetic and pharmacological interventions toward CatK activity ameliorate SMC apoptosis in vitro and in vivo. Thus, these findings indicate that the ability of increased CatK activity to activate pro-caspase-8 is a crucial step to induce SMC apoptosis in response to oxidative stress, which is linked to the apoptotic dying cells-derived growth signaling and SMC proliferation event under our experimental conditions.

Human and animal atherosclerotic lesions contain extensive expression of TLR2 protein.^{18,19} Accumulating evidence shows that TLR2 activates caspase-8-related apoptosis signaling pathways in several cell lines.^{20,23,46} Here, siTLR2 suppressed increased caspase-8 expression in response to oxidative apoptotic stress in cultured SMCs. As compared with controls, our observations here show that both siTLR2 and siCasp8 mitigated expression of PLF-1 protein in vitro, indicating that TLR2-dependent caspase-8 signaling may be required in regulation of PLF-1 expression in vascular SMCs. In addition, in the data presented here, injured carotid arterial tissues had decreased levels of TLR2 protein as well as

caspase-8 protein in CatK^{-/-} mice as compared with CatK^{+/+} mice. Likewise, CatK deletion suppressed both protein expressions in cultured SMCs. Furthermore, we observed that inhibition of CatK activity resulted in decreased levels of PLF-1 protein in plasma and injured carotid arterial tissues. Taken together, these findings lead us to consider that modulation of TLR2-dependent caspase-8 expression and activation by CatK inhibition using genetic and pharmacological approaches is responsible for regulation of PLF-1 production and secretion, which is crucial for the apoptotic dying cells-derived cellular growth signal and proliferative action under our experimental conditions. It should be noted that although there is not any evidence, the CatK deletion-mediated decrease in oxidative stress and inflammation might be a negative feedback effect to reduce TLR2 expression.

Our findings demonstrated the potential efficacy of PLF-1 blocking antibody in the management of vascular remodeling after injuries. Based on our findings of mouse recombinant PLF-1 administration experiments, we propose that PLF-1 might be a potential molecular target for tissue wound healing and regeneration.²⁹ Another implication of our animal study is the potential use of increased circulating PLF-1 as a novel biomarker for vascular injury.

Conclusions

This newly discovered PLF-1-mediated neointimal hyperplasia pathway has profound implications for the understanding of vascular biology and restenosis management after established endovascular therapies. Our present findings demonstrate a key role for cell apoptosis in promoting tissue remodeling to injury, leading us to propose to name this mechanism the “dying instinctively switches on new growth” pathway of tissue replacement and remodeling. Based on the results of other studies^{7,42} and our own findings, we contend that this is a fundamental biological process (affecting wound healing, cancer therapy, and endovascular therapy) by which metazoan organisms use cell damage and start replacing cells by regeneration, repair, or mixed processes. The presence of such a cascade pathway appears to exhibit an inextricable and unique link between the “yin and yang” of cellular apoptosis and life in animals and humans.

Sources of Funding

This work was supported, in part, by the National Natural Science Foundation of China (NSFC, CHINA) (Nos. 81260068, 81560240, 81660240, 81770485, 81760091, and AD19120092) and by grants from the Japan Society for the Promotion of Science (JSPS, JAPAN) (Nos. 15H04801, 15H04802). In addition, Hu is a

postdoctoral fellow of the Japan Society for the Promotion of Science (JSPS, JAPAN) (No. 26-04418).

Disclosures

None.

References

- Sopko G. Preventing cardiac events and restenosis after percutaneous coronary intervention. *JAMA*. 2002;287:3259–3261.
- Juni RP, Duckers HJ, Vanhoutte PM, Virmani R, Moens AL. Oxidative stress and pathological changes after coronary artery interventions. *J Am Coll Cardiol*. 2013;61:1471–1481.
- Durand E, Mallat Z, Addad F, Vilde F, Desnos M, Guerot C, Tedgui A, Lafont A. Time courses of apoptosis and cell proliferation and their relationship to arterial remodeling and restenosis after angioplasty in an atherosclerotic rabbit model. *J Am Coll Cardiol*. 2002;39:1680–1685.
- Hu L, Cheng XW, Song H, Inoue A, Jiang H, Li X, Shi GP, Kozawa E, Okumura K, Kuzuya M. Cathepsin K activity controls injury-related vascular repair in mice. *Hypertension*. 2014;63:607–615.
- Deuse T, Hua X, Wang D, Maegdefessel L, Heeren J, Scheja L, Bolanos JP, Rakovic A, Spin JM, Stubbendorff M, Ikeno F, Langer F, Zeller T, Schulte-Uentrop L, Stoehr A, Itagaki R, Haddad F, Eschenhagen T, Blankenberg S, Kiefmann R, Reichenspurner H, Velden J, Klein C, Yeung A, Robbins RC, Tsao PS, Schrepfer S. Dichloroacetate prevents restenosis in preclinical animal models of vessel injury. *Nature*. 2014;509:641–644.
- Tasaki T, Yamada S, Guo X, Tanimoto A, Wang KY, Nabeshima A, Kitada S, Noguchi H, Kimura S, Shimajiri S, Kohno K, Ichijo H, Sasaguri Y. Apoptosis signal-regulating kinase 1 deficiency attenuates vascular injury-induced neointimal hyperplasia by suppressing apoptosis in smooth muscle cells. *Am J Pathol*. 2013;182:597–609.
- Huang Q, Li F, Liu X, Li W, Shi W, Liu FF, O'Sullivan B, He Z, Peng Y, Tan AC, Zhou L, Shen J, Han G, Wang XJ, Thorburn J, Thorburn A, Jimeno A, Raben D, Bedford JS, Li CY. Caspase 3-mediated stimulation of tumor cell repopulation during cancer radiotherapy. *Nat Med*. 2011;17:860–866.
- Obenauf AC, Zou Y, Ji AL, Vanharanta S, Shu W, Shi H, Kong X, Bosenberg MC, Wiesner T, Rosen N, Lo RS, Massague J. Therapy-induced tumour secretomes promote resistance and tumour progression. *Nature*. 2015;520:368–372.
- Turk B, Turk D, Turk V. Lysosomal cysteine proteases: more than scavengers. *Biochim Biophys Acta*. 2000;1477:98–111.
- Wang B, Sun J, Kitamoto S, Yang M, Grubb A, Chapman HA, Kalluri R, Shi GP. Cathepsin S controls angiogenesis and tumor growth via matrix-derived angiogenic factors. *J Biol Chem*. 2006;281:6020–6029.
- Cheng XW, Shi GP, Kuzuya M, Sasaki T, Okumura K, Murohara T. Role for cysteine protease cathepsins in heart disease: focus on biology and mechanisms with clinical implication. *Circulation*. 2010;125:1551–1562.
- Kozawa E, Nishida Y, Cheng XW, Urakawa H, Arai E, Futamura N, Shi GP, Kuzuya M, Hu L, Sasaki T, Ishiguro N. Osteoarthritic change is delayed in a Ctsk-knockout mouse model of osteoarthritis. *Arthritis Rheum*. 2012;64:454–464.
- Sun J, Sukhova GK, Zhang J, Chen H, Sjoberg S, Libby P, Xia M, Xiong N, Gelb BD, Shi GP. Cathepsin K deficiency reduces elastase perfusion-induced abdominal aortic aneurysms in mice. *Arterioscler Thromb Vasc Biol*. 2012;32:15–23.
- Jiang H, Cheng XW, Shi GP, Hu L, Inoue A, Yamamura Y, Wu H, Takeshita K, Li X, Huang Z, Song H, Asai M, Hao CN, Unno K, Koike T, Oshida Y, Okumura K, Murohara T, Kuzuya M. Cathepsin K-mediated Notch1 activation contributes to neovascularization in response to hypoxia. *Nat Commun*. 2014;5:3838.
- Sukhova GK, Shi GP, Simon DI, Chapman HA, Libby P. Expression of the elastolytic cathepsins S and K in human atheroma and regulation of their production in smooth muscle cells. *J Clin Invest*. 1998;102:576–583.
- Cheng XW, Kuzuya M, Sasaki T, Arakawa K, Kanda S, Sumi D, Koike T, Maeda K, Tamaya-Mori N, Shi GP, Saito N, Iguchi A. Increased expression of elastolytic cysteine proteases, cathepsins S and K, in the neointima of balloon-injured rat carotid arteries. *Am J Pathol*. 2004;164:243–251.
- Hua Y, Zhang Y, Dolence J, Shi GP, Ren J, Nair S. Cathepsin K knockout mitigates high-fat diet-induced cardiac hypertrophy and contractile dysfunction. *Diabetes*. 2013;62:498–509.
- Edfeldt K, Swedenborg J, Hansson GK, Yan ZQ. Expression of Toll-like receptors in human atherosclerotic lesions: a possible pathway for plaque activation. *Circulation*. 2002;105:1158–1161.

19. Cheng XW, Song H, Sasaki T, Hu L, Inoue A, Bando YK, Shi GP, Kuzuya M, Okumura K, Murohara T. Angiotensin type 1 receptor blocker reduces intimal neovascularization and plaque growth in apolipoprotein E-deficient mice. *Hypertension*. 2011;57:981–989.
20. Into T, Kiura K, Yasuda M, Kataoka H, Inoue N, Hasebe A, Takeda K, Akira S, Shibata K. Stimulation of human Toll-like receptor (TLR) 2 and TLR6 with membrane lipoproteins of *Mycoplasma fermentans* induces apoptotic cell death after NF-kappa B activation. *Cell Microbiol*. 2004;6:187–199.
21. Schmidt L, Carrillo-Sepulveda MA. Toll-like receptor 2 mediates vascular contraction and activates RhoA signaling in vascular smooth muscle cells from STZ-induced type 1 diabetic rats. *PLoS One*. 2015;10:e012374.
22. Lee GL, Chang YW, Wu JY, Wu ML, Wu KK, Yet SF, Kuo CC. TLR 2 induces vascular smooth muscle cell migration through cAMP response element-binding protein-mediated interleukin-6 production. *Arterioscler Thromb Vasc Biol*. 2012;32:2751–2760.
23. Lemmers B, Salmena L, Bidere N, Su H, Matysiak-Zablocki E, Murakami K, Ohashi PS, Jurisicova A, Lenardo M, Hakem R, Hakem A. Essential role for caspase-8 in Toll-like receptors and NFkappaB signaling. *J Biol Chem*. 2007;282:7416–7423.
24. Linzer DI, Lee SJ, Ogren L, Talamantes F, Nathans D. Identification of proliferin mRNA and protein in mouse placenta. *Proc Natl Acad Sci USA*. 1985;82:4356–4359.
25. Lee SJ, Nathans D. Proliferin secreted by cultured cells binds to mannose 6-phosphate receptors. *J Biol Chem*. 1988;263:3521–3527.
26. Toft DJ, Rosenberg SB, Bergers G, Volpert O, Linzer DI. Reactivation of proliferin gene expression is associated with increased angiogenesis in a cell culture model of fibrosarcoma tumor progression. *Proc Natl Acad Sci USA*. 2001;98:13055–13059.
27. Groskopf JC, Syu LJ, Saltiel AR, Linzer DI. Proliferin induces endothelial cell chemotaxis through a G protein-coupled, mitogen-activated protein kinase-dependent pathway. *Endocrinology*. 1997;138:2835–2840.
28. Wang XY, Yin Y, Yuan H, Sakamaki T, Okano H, Glazer RI. Musashi 1 modulates mammary progenitor cell expansion through proliferin-mediated activation of the Wnt and Notch pathways. *Mol Cell Biol*. 2008;28:3589–3599.
29. Yang X, Qiao D, Meyer K, Pier T, Keles S, Friedl A. Angiogenesis induced by signal transducer and activator of transcription 5A (STAT5A) is dependent on autocrine activity of proliferin. *J Biol Chem*. 2012;287:6490–6502.
30. Kuzuya M, Kanda S, Sasaki T, Tamaya-Mori N, Cheng XW, Itoh T, Itohara S, Iguchi A. Deficiency of gelatinase a suppresses smooth muscle cell invasion and development of experimental intimal hyperplasia. *Circulation*. 2003;108:1375–1381.
31. Sasaki T, Kuzuya M, Nakamura K, Cheng XW, Shibata T, Sato K, Iguchi A. A simple method of plaque rupture induction in apolipoprotein E-deficient mice. *Arterioscler Thromb Vasc Biol*. 2006;26:1304–1309.
32. Burger D, Kwart DG, Montezano AC, Read NC, Kennedy CR, Thompson CS, Touyz RM. Microparticles induce cell cycle arrest through redox-sensitive processes in endothelial cells: implications in vascular senescence. *J Am Heart Assoc*. 2012;1:e001842. DOI: 10.1161/JAHA.112.001842.
33. Cheng XW, Kuzuya M, Kim W, Song H, Hu L, Inoue A, Nakamura K, Di Q, Sasaki T, Tsuzuki M, Shi GP, Okumura K, Murohara T. Exercise training stimulates ischemia-induced neovascularization via phosphatidylinositol 3-kinase/Akt-dependent hypoxia-induced factor-1 alpha reactivation in mice of advanced age. *Circulation*. 2012;122:707–716.
34. Cheng XW, Murohara T, Kuzuya M, Izawa H, Sasaki T, Obata K, Nagata K, Nishizawa T, Kobayashi M, Yamada T, Kim W, Sato K, Shi GP, Okumura K, Yokota M. Superoxide-dependent cathepsin activation is associated with hypertensive myocardial remodeling and represents a target for angiotensin II type 1 receptor blocker treatment. *Am J Pathol*. 2008;173:358–369.
35. Iwata K, Ikami K, Matsuno K, Yamashita T, Shiba D, Ibi M, Matsumoto M, Katsuyama M, Cui W, Zhang J, Zhu K, Takei N, Kokai Y, Ohneda O, Yokoyama T, Yabe-Nishimura C. Deficiency of NOX1/nicotinamide adenine dinucleotide phosphate, reduced form oxidase leads to pulmonary vascular remodeling. *Arterioscler Thromb Vasc Biol*. 2014;34:110–119.
36. Tang X, Guo Y, Nakamura K, Huang H, Hamblin M, Chang L, Villacorta L, Yin K, Ouyang H, Zhang J. Nitroalkenes induce rat aortic smooth muscle cell apoptosis via activation of caspase-dependent pathways. *Biochem Biophys Res Commun*. 2010;397:239–244.
37. Parfett C, Macmillan J, Pilon R. Oxidative stress mediates tumor promoter-induced proliferin gene-expression in c3h10t1/2 cells. *Int J Oncol*. 1993;3:917–925.
38. Jackson D, Volpert OV, Bouck N, Linzer DI. Stimulation and inhibition of angiogenesis by placental proliferin and proliferin-related protein. *Science*. 1994;266:1581–1584.
39. Leksa V, Pfisterer K, Ondrovicova G, Binder B, Lakatosova S, Donner C, Schiller HB, Zwirzitz A, Mrvova K, Pevala V, Kutejova E, Stockinger H. Dissecting mannose 6-phosphate-insulin-like growth factor 2 receptor complexes that control activation and uptake of plasminogen in cells. *J Biol Chem*. 2012;287:22450–22462.
40. El-Shewy HM, Luttrell LM. Insulin-like growth factor-2/mannose-6 phosphate receptors. *Vitam Horm*. 2009;80:667–697.
41. Qin C, Liu Z. In atherosclerosis, the apoptosis of endothelial cell itself could directly induce over-proliferation of smooth muscle cells. *Med Hypotheses*. 2007;68:275–277.
42. Li F, Huang Q, Chen J, Peng Y, Roop DR, Bedford JS, Li CY. Apoptotic cells activate the “phoenix rising” pathway to promote wound healing and tissue regeneration. *Sci Signal*. 2010;3:ra13.
43. Earnshaw WC, Martins LM, Kaufmann SH. Mammalian caspases: structure, activation, substrates, and functions during apoptosis. *Annu Rev Biochem*. 1999;68:383–424.
44. Gross A, McDonnell JM, Korsmeyer SJ. BCL-2 family members and the mitochondria in apoptosis. *Genes Dev*. 1999;13:1899–1911.
45. Boatright KM, Salvesen GS. Caspase activation. *Biochem Soc Symp*. 2003;70:233–242.
46. Aliprantis AO, Yang RB, Weiss DS, Godowski P, Zychlinsky A. The apoptotic signaling pathway activated by Toll-like receptor-2. *EMBO J*. 2000;19:3325–3336.